Sound & Vibration 2026, 60(6), 4817.
doi: https://doi.org/10.59400/sv4817

Article

Response of a cylindrical shell with a solid viscoelastic filler to a non-axisymmetric moving load

Zafar Boltayev[1], Nuriddin Esanov[2], Shuhrat Jurayev[3,*], Rano Sabirova[1], Gulzira Mirzoyeva[1], Uchqun Safarov[4], Sherali Khamidov[3], Anora Jumayeva[5], Sitorabonu Otajonova[1], Kamola Khaydarova[6], Nazokat Ergasheva[1]

[1] Department of Exact Sciences, Bukhara State Technical University, Bukhara 200117, Uzbekistan; boltayev_zafar@bstu.uz (ZB); sabirova_rano@bstu.uz (RS); gmirzoeva@bstu.uz (GM); sotajonova@bstu.uz (SO); nergasheva@bstu.uz (NE)

[2] Department of Pedagogy and Psychology, Asia International University, Bukhara 200100, Uzbekistan; esanovnuriddin@oxu.uz

[3] Department of Mathematics and Informatics, Bukhara State Pedagogical Institute, Bukhara 200130, Uzbekistan; hamidovsherali1985@buxdpi.uz

[4] Department of Structural Mechanics and Earthquake Engineering, Tashkent University of Architecture and Civil Engineering, Tashkent 100194, Uzbekistan; u.safarov@taqu.uz

[5] Department of Architecture and Construction, Samarkand State Institute of Architecture and Civil Engineering, Samarkand 140143, Uzbekistan; anora.jumayeva@samdaqu.edu.uz

[6] Department of Theoretical and Engineering Mechanics, Samarkand State University, Samarkand 140104, Uzbekistan; xaydarovakamola92@samdu.uz

* **Corresponding author:** Shuhrat Jurayev, jurayev_shuhrat@buxdpi.uz

CITATION

Boltayev Z, Esanov N, Jurayev S, et al. Response of a cylindrical shell with a solid viscoelastic filler to a non-axisymmetric moving load. Sound & Vibration. 2026; 60(6): 4817. https://doi.org/10.59400/sv4817

ARTICLE INFO

Received: 12 June 2026
Revised: 16 July 2026
Accepted: 24 August 2026
Available online: 3 September 2026

Abstract: This paper examines the response of a cylindrical shell with a solid viscoelastic core to a non-axisymmetric moving load. We formulate the problem of determining the stationary stress-strain state of a shell with a solid multilayer viscoelastic core when a non-axisymmetric normal load moves along an infinitely long cylindrical shell filled with a continuous viscoelastic inertial core. The equation of motion of the shell is described by shell equations subject to the Kirchhoff–Love hypotheses, while the motion of the core is described by the dynamic equations of the theory of elasticity. Sliding-contact conditions are satisfied at the interface between the shell and the core. The problem is solved in a moving coordinate system using the Fourier transform and the introduction of potential functions, which in the transform space are represented as Fourier series. The solution is obtained in terms of special Bessel and Neumann functions of a complex argument. Numerical results were obtained using the MATLAB software environment. On the basis of the numerical results obtained, it is established that, moving away from the point of load application along the length of the shell, the distribution pattern changes substantially, especially for the stresses. Separation of the shell from the core can occur not only around the circumference but also along the length, and the variation of the core stiffness within the range considered here has little effect on the length of the contact zone.

Keywords: cylindrical shell; viscoelastic core; Bessel and Neumann functions; Fourier transform; contact zone

1. Introduction

The action of a moving load on flat and cylindrical structures is of great practical importance [1,2]. For example, at a certain load velocity, called the critical velocity, a resonance phenomenon occurs in which the deflection of the elastic layer increases, which can lead to failure of the plate structure.

Studies [3, 4] consider an elastic layer on an elastic foundation, along which a load moves at a constant velocity. The first part of the work studies a one-dimensional formulation of the problem: an infinite elastic beam on a Winkler foundation under a constant load moving uniformly, i.e., at a constant velocity. An exact value of the beam deflection is obtained, and the critical velocity is found.

The second part of the work investigates a two-dimensional formulation of the problem. The Mindlin system of equations [5] is taken as the model for the elastic layer, while the equations of the theory of elasticity for the plane-strain state are used to describe the elastic foundation. The coupling condition between them is sliding contact [6,7]. A solution for a concentrated load as a function of moving coordinates is obtained [8]. The condition for the onset of resonance reduces to a nonlinear algebraic equation. The smallest positive root of the equation is the critical velocity.

Many loads acting on solid bodies and structures are functions of both time and space, and also move at variable velocity [9, 10]. In the work of Firsanov [11], the dynamic responses of "homogeneous" beams subjected to moving loads were obtained by analytical methods. In numerous studies, various methods were used to solve the problem of vibrations of a "homogeneous" flat plate, freely supported on its edges, under a load moving along a prescribed trajectory [12,13].

In the work of Zhou et al. and Auersch [14, 15], the dynamic behavior of a road bridge and the ground was studied by the method of full-scale field tests. Also, in studies by Karpov et al. and Wang et al. [16, 17], nonlinear effects were investigated in the problem of a beam on a foundation under a "moving load," together with the transient solution for a cylindrical shell under the action of an enveloping axisymmetric pressure wave.

Most of the solutions cited above were based on analytical methods. However, for the most complex engineering problems, closed-form analytical solutions are very difficult to obtain. In the articles of Hussein and Hunt, and Bahranifard et al. [18,19], numerical methods were applied to solve the problem of the response of a cylindrical shell with a core to a moving load. In problems on the action of moving loads, the analysis is usually restricted to pre-resonance velocities of motion [20,21].

In the present work, two methods are developed for solving stationary dynamic problems for arbitrary constant velocities of load motion, conventionally referred to here as the contour-deformation (integration-contour) method and the damping method.

The first method is applied to systems without energy dissipation, and the second to the case when the system contains a mechanism of natural damping of various physical origins [22, 23]. This mechanism may consist in the transfer of energy from a plate or shell excited by a supersonically moving load to infinity by expansion-wave components in a liquid or an elastic medium of unbounded extent; its presence may be explained by energy dissipation in the material of the shell itself; and, finally, damping appears when the viscoelastic properties of the core are taken into account.

The first method is based on isolating the singularities in the integrand, deforming the integration contour, and using a special algorithm for computing the integral along such a contour. In the second method, the improper integrals in the inversion formulas have no singularities on the real axis [24, 25]. The solution obtained by this approach is unique for any magnitude of the load velocity, and the algorithm for obtaining numerical results is analogous to that used previously for pre-resonance velocities. Using the methods developed, the influence of the constant velocity of load motion on the stationary dynamic behavior of two- and three-layer cylindrical shells was investigated.

In Girnis's study [26], the problem of the action on the inner surface of an infinitely long elastic cylindrical shell of a load moving uniformly along its axis was studied. The load acting on the inner surface of the shell is harmonic along its axis. The layered shell is situated in an elastic space. The motion of the elastic medium and of the shell layers is described by the dynamic equations of the theory of elasticity in terms of Lame potentials. The potentials of the longitudinal and transverse waves are described as Fourier-Bessel series, and the unknown integration constants are determined from the boundary conditions.

On the basis of the numerical results, it is established that, as the distance from the surface of the cavity increases, the influence of the dynamic action of the moving load on the medium decreases.

The basic model problems studied concern the dynamics of transport in underground structures [27–29]. These are problems of the action of a transport load on the circular surface of a tunnel. The load is applied over a limited region and moves along the inner surface forming its plane. It is assumed that the objects under consideration are located in an elastic half-space. A cylindrical shell in an elastic space is considered in the studies of Li et al. and Guo and Pan [30, 31], respectively. Numerical results are obtained as a function of the properties of the surrounding soil.

The present work is devoted to studying the response of a cylindrical shell with a solid viscoelastic core to a non-axisymmetric moving load. The problem is solved analytically, but the Gauss and Muller methods are used to obtain the numerical results.

2. Statement of the problem and solution methods

We consider the problem of the action of a normal load moving at constant velocity on a cylindrical shell with a viscoelastic core. An infinite, uniformly distributed radial load moves over the outer surface of the cylinder at a constant velocity V. The basic equations of motion of the multilayer core are given in the form [32]

$$\widetilde{\mu}_n \nabla^2 \overrightarrow{u} + \left(\widetilde{\lambda}_n + \widetilde{\mu}_n\right) \text{grad div } \overrightarrow{u} = \rho_n \frac{\partial^2 \overrightarrow{u}}{\partial t^2}, \qquad (n = 1, 2, 3 \ldots) \tag{1}$$

Here, $u_n(u_{xn},\ u_{yn},\ u_{zn})$ is the displacement vector of points of the *n*-th cylinder; ρ_n is the density of the *n*-th cylinder;

$$\widetilde{\lambda}_n \varphi(t) = \frac{\nu_n \widetilde{E}_n \varphi(t)}{(1+\nu_n)(1-2\nu_n)}; \qquad \widetilde{\mu}_n \varphi(t) = \frac{\nu_n \widetilde{E}_n \varphi(t)}{2(1+\nu_n)},$$

ν_n is the Poisson ratio of the *n*-th cylinder, $\varphi(t)$ is an arbitrary function of time.

If the Koltunov–Rzhanitsyn relaxation kernel is used instead of (1), then the elastic modulus is replaced by operators, i.e., $\widetilde{E}_n$ the operator elastic modulus has the form [32]:

$$\widetilde{E}_n\varphi(t) = E_{0n}\left[\varphi(t) - \int_0^t R_{E_n}(t-\tau)\varphi(t)\,d\tau\right] \tag{2}$$

$R_{E_n}(t-\tau)$ is the relaxation kernel; ν_n is the Poisson ratio, E_{0n} is the instantaneous elastic modulus. The relationship between stresses and strains has the following form [32]:

$$\sigma_{ij}^{(n)} = \widetilde{\lambda}_n\widetilde{\varepsilon}_{kk}^{(n)}\delta_{ij} + 2\widetilde{\mu}_n\widetilde{\varepsilon}_{ij}^{(n)}$$

At the contact surface $r = R_1$ and the free surface of the cylinder $r = R_0$ and $r = R_2$:

$$\begin{gathered}
\sigma_{rr}^{(1)}\Big|_{r=R_0} = \sigma_{r\theta}^{(1)}\Big|_{r=R_0} = \sigma_{rz}^{(1)}\Big|_{r=R_0} = 0, \\
\sigma_{rr}^{(2)}\Big|_{r=R_2} = \sigma_{r\theta}^{(2)}\Big|_{r=R_2} = \sigma_{rz}^{(2)}\Big|_{r=R_2} = 0, \\
\sigma_{rr}^{(1)}\Big|_{r=R_1} = \sigma_{rr}^{(2)}\Big|_{r=R_1}, \quad \sigma_{r\theta}^{(1)}\Big|_{r=R_1} = \sigma_{r\theta}^{(2)}\Big|_{r=R_1}, \quad \sigma_{rz}^{(1)}\Big|_{r=R_1} = \sigma_{rz}^{(2)}\Big|_{r=R_1}, \\
u_{r1}|_{r=R_1} = u_{r2}|_{r=R_1}, \quad u_{\theta1}|_{r=R_1} = u_{\theta2}|_{r=R_1}, \quad u_{z1}|_{r=R_1} = u_{z2}|_{r=R_1}.
\end{gathered} \tag{3}$$

To solve the integro-differential equation above on the basis of the boundary conditions, assuming that the integral terms in them are small, the freezing method developed by Filatov and Sancheleev and presented in Gao et al. and Safarov et al.'s articles [4,32] can be used. Then relations are replaced by the approximate relations of the form

$$\begin{gathered}
\overline{\lambda}_n = \lambda_{0n}\Gamma_{En}; \bar{\mu}_n = \mu_{0n}\Gamma_{En}, \\
\lambda_{0n} = \frac{v_n E_{0n}}{(1+v_n)(1-2v_n)}, \mu_{0n} = \frac{v_n E_{0n}}{2(1+v_n)}. \\
\Gamma_{En} = 1 - \Gamma_{En}^c(\omega_R) - i\Gamma_{En}^s(\omega_R), \\
\Gamma_{En}^c(\omega_R) = \int_0^\infty R_{En}(\tau)\cos\omega_R\tau d\tau, \Gamma_{En}^s(\omega_R) = \int_0^\infty R_{En}(\tau)\sin\omega_R\tau d\tau,
\end{gathered} \tag{4}$$

$\lambda_{0n},\ \mu_{0n}$ are the instantaneous Lame coefficients, $n = 1, 2$, $R_{En}(t)$ is the relaxation kernel, ω_R is the real part of the complex frequency.

In the calculations, the three-parameter Koltunov–Rzhanitsyn relaxation kernel was used: $R_{En}(t) = A_n e^{-b_n t}/t^{1-a_n}$. The parameters of the relaxation kernel are given in the monograph [33].

To study the propagation of eigenwaves, a dispersion equation was constructed. In this case, the external load is not taken into account, so the initial conditions are taken to be homogeneous.

In some cases, to simplify the calculations, instead of the shell, the theory of shells based on the Kirchhoff–Love hypothesis (or the Timoshenko hypothesis) is used. Then, for $n = 1$, a thin viscoelastic shell is used, which is described by the equation of motion of a viscoelastic shell subject to the Kirchhoff–Love hypotheses [34]:

$$\bar{G}_0[L]\overrightarrow{u} = \frac{1-\nu_0^2}{E_0 h_0}\overrightarrow{p} + \rho_0\frac{1-\nu_0^2}{E_0}\frac{\partial^2\overrightarrow{u}}{\partial t^2}, \tag{5}$$

where $\overrightarrow{u}(u, J, w)$ are the displacements of points of the shell (or pipe), h_0 is the shell thickness, ρ_0 is the density, n_0 is Poisson's ratio, E_0 is the instantaneous elastic modulus, $\frac{1}{p}$ is the load acting from the side of the core, $\left[\bar{L}\right]$ is the differential operator (according to the Kirchhoff–Love theory):

$$\bar{G}_0\left[\bar{L}\right]=\bar{G}_0\begin{bmatrix} \frac{\partial^2}{\partial x^2}+\frac{1-n_0}{2R_1^2}\frac{\partial^2}{\partial\theta^2} & \frac{1+n_0}{2R_1}\frac{\partial^2}{\partial x\partial\theta} & \frac{n_0}{R_1}\frac{\partial}{\partial x} \\ \frac{1+n_0}{2R_1}\frac{\partial^2}{\partial x\partial\theta} & \frac{1-n_0}{2}(1+4a)\frac{\partial^2}{\partial x^2}+\frac{1}{R_1^2}(1+a)\frac{\partial^2}{\partial\theta^2} & \frac{1}{R_1^2}\frac{\partial}{\partial\theta}-a\left(2-n_0\right)\frac{\partial^3}{\partial x^2\partial\theta}-\frac{a}{R_1^2}\frac{\partial^3}{\partial\theta^3} \\ \frac{n_0}{R_1}\frac{\partial}{\partial x} & \frac{1}{R_1^2}\frac{\partial}{\partial\theta}-a\left(2-n_0\right)\frac{\partial^3}{\partial x^2\partial\theta}-\frac{a}{R_1^2}\frac{\partial^3}{\partial\theta^3} & \frac{1}{R_1^2}+a\left(\frac{\partial^2}{\partial x^2}+\frac{1}{R_1^2}\frac{\partial^2}{\partial\theta^2}\right)^2 \end{bmatrix}$$

$$\bar{G}_0=1-G^c_{E1}\left(\omega_R\right)+iG^s_{E1}\left(\omega_R\right),$$

$$G^c_{E1}\left(\omega_R\right)=\int_0^t R_{E1}(t)\cos\omega_R t\,dt,\qquad G^s_{E1}\left(\omega_R\right)=\int_0^t R_{E1}(t)\sin\omega_R t\,dt,\qquad a=\frac{h_0^2}{12R_1^2},$$

$R_{E1}(t)$ is the relaxation kernel. The paper presents a study of the stress-strain state of the core and shells under the action of moving loads. The shell is considered according to three theories:

1. According to the Kirchhoff–Love theory; 2. According to the Timoshenko theory; 3. According to the three-dimensional theory of viscoelasticity. A comparative analysis is presented.

The motion of the viscoelastic core, taking (4) into account, is described by the dynamic equations of the theory of elasticity

$$\bar{\mu}_k C^2\nabla^2\overrightarrow{u}+\left(\bar{\lambda}_k+\bar{\mu}_k\right)\text{grad div}\,\overrightarrow{u}=\rho_k\frac{\partial^2\overrightarrow{u}}{\partial t^2},\qquad (k=1,2,3,\ldots,N). \tag{6}$$

where $\bar{\mu}\left(u_r,u_j,u_x\right)$ are the displacements of points of the core, ρ_k is the density of the material. If the hollow core is single-layer (n = 1), then at the contact between the shell and the core, the sliding-contact conditions are satisfied

$$\sigma_{rx}=\sigma_{r\theta}=0;\sigma_{rr}=-q_{rc};u_r=w\left(r=R_1\right). \tag{7}$$

To solve the equation for the core, the method of potentials is applied, and the differential equation of the problem under consideration is reduced to the wave equation [32]

$$\nabla^2\Phi=\frac{1}{c_p^2}\frac{\partial^2\Phi}{\partial t^2};\qquad\nabla^2\Psi=\frac{1}{c_s^2}\frac{\partial^2\Psi}{\partial t^2};\qquad\nabla^2X=\frac{1}{c_s^2}\frac{\partial^2X}{\partial t^2}. \tag{8}$$

Here

$$\bar{c}_p^2=c_{p0}^2\Gamma_{En},c_{p0}^2=\left(\lambda_0+2\mu_0\right)/\rho,$$
$$\bar{c}_s^2=c_{s0}^2\Gamma_{En},c_{s0}^2=\mu_0/\rho.$$

Let us apply the Fourier transform in the moving coordinate system to (8) with respect to $\eta(=(x-ct)/H)$ [32]

$$\bar{j}(x)=\int_{-\Gamma}^{\Gamma}F(h)e^{-ixh}\,dh;\qquad F(h)=\frac{1}{2\pi}\int_{-\Gamma}^{\Gamma}\bar{j}_k(x)e^{ixh}\,dx.$$

In the transform space, the solution of the transformed equations is sought as Fourier series in the angular coordinate q, assuming that the transforms of the given normal load are expanded in Fourier series in q and we introduce potential functions, which in the transform space are represented as Fourier series:

$$\{\Phi, \Psi\} = \sum_{n=0}^{\infty} \{\varphi_n, \psi_n\} \cos(n\theta); \qquad X = \sum_{n=1}^{\infty} \chi_n \sin(n\theta), \tag{9}$$

moreover, the Fourier coefficients of the displacement components in the core are related to the harmonics of the potential functions by the relations:

$$\begin{gathered} U_n(r) = i\xi\varphi_n + \tfrac{d^2\psi_n}{dr^2} + \tfrac{1}{r}\tfrac{d\psi_n}{dr} - \tfrac{n^2}{r^2}\psi_n, \\ V_n(r) = -\tfrac{n}{r}\varphi_n + i\xi\tfrac{n}{r}\psi_n - \tfrac{d\chi_n}{dr}, \\ W_n(r) = \tfrac{d\varphi_n}{dr} - i\xi\tfrac{d\psi_n}{dr} + \tfrac{n}{r}\chi_n. \end{gathered}$$

In this case, j_n, y_n, c_n are obtained from, whose solutions for the case of a solid core, for load velocities smaller than the shear-wave propagation velocity, $c < c_s$, have the form

$$\begin{gathered} \varphi_n\left(r_*, \xi\right) = B_n(\xi) I_n\left(m\xi r_*\right); \psi_n\left(r_*, \xi\right) = D_n(\xi) I_n\left(m_s\xi r_*\right); \\ x_n\left(r_*, \xi\right) = S_n(\xi) I_n\left(m_s\xi r_*\right). \end{gathered} \tag{10}$$

where

$$m = \sqrt{1 - M_p^2}, m_s = \sqrt{1 - M_s^2}, M_p^2 = \frac{c}{c_p\Gamma_p\left(\omega_R\right)}, M_s^2 = \frac{c}{c_s\Gamma_s\left(\omega_R\right)}$$

$$\overline{m} = \sqrt{M_p^2 - 1}, \overline{m}_s = \sqrt{M_s^2 - 1}, \rho^{\cdot} = \rho_1/\rho_2, k_1 = h/b,$$

$$c_p = \left[\frac{2G_{20}\left(1 - \nu_{02}\right)}{\rho_2\left(1 - 2\nu_{02}\right)}\right]^{1/2}, c_s = \left[\frac{G_{20}}{\rho_2}\right]^{1/2}, \gamma = G_{10}/G_{20}.$$

Substituting (10) into (8) and satisfying the boundary conditions, in the transform space, we obtain the following relation between the reaction of the core and the radial displacements of the shell:

$$\begin{gathered} q_{ri,n}^0 = G_c k f_1(\xi, n, c)\tfrac{w_n^0}{h}; \\ f_1(\xi, n, c) = \tfrac{e_3 d_1 + 2e_4 - 2(e_2 - 1)d_2}{e_1 d_1 + m_s^2 e_2}; \\ e_1 = n + m\xi\tfrac{I_{n+1}(m\xi)}{I_n(m\xi)}; \qquad e_2 = n + m_s\xi\tfrac{I_{n+1}(m_s\xi)}{I_n(m_s\xi)}; \\ e_3 = \left(1 + m_s^2\right)\xi^2 + 2n^2 - 2e_1; \qquad e_4 = m_s^2\xi^2 + n^2 - e_2; \\ e_5 = n^2 + \tfrac{m_s^2\xi^2}{2} - e_2; \qquad d_2 = 2e_1 d_1 + \left(1 + m_s^2 e_2\right); \\ d_1 = \tfrac{n^2(e_2 - 1) - \left(1 + m_s^2\right)e_2 e_5}{2e_1 e_5 - n^2(e_1 - 1)}. \end{gathered} \tag{11}$$

Substituting (8) into the transformed equations of motion of the shell, we obtain a system of algebraic equations with respect to u_n^0, v_n^0, ω_n^0 whose general solution can be written in the form

$$\begin{gathered}\{u_n^0, v_n^0, w_n^0\} = -\tfrac{1-\nu}{2Gk^2} p_{r,n}^0 \tfrac{\{V_1, V_2, V_3\}}{\det_n \|a_{k,l}\|};\\ d_{11} = -\left(1 - \tfrac{1-\nu}{3} c_0^2\right) \xi^2 - \tfrac{(1-\nu)n^2}{2};\\ d_{12} = d_{21} = i\xi \tfrac{(1+\nu)n}{2}; \qquad d_{13} = d_{31} = i\nu\xi;\\ d_{22} = \tfrac{1-\nu}{2}\left(1 - \tfrac{2}{3} c_0^2\right) \xi^2 + n^2; \qquad d_{23} = d_{32} = n;\\ d_{33} = \tfrac{k^2}{12}\left(n^2 + \xi^2\right)^2 + 1 - \tfrac{1-\nu}{3} c_0^2 \xi^2 - \tfrac{1-\nu}{2k\gamma} f_1(\xi, n, c).\end{gathered} \tag{12}$$

The determinants $\Delta_j (j = 1, 2, 3)$ are obtained from $\det\limits_n \|d_{k2}\|$ by replacing the j-th column with a column having elements $\{0, 0, 1\}$. Similarly to [32,33]

$$\begin{gathered}q_{r,n}^0 = -\tfrac{1-\nu}{3} \tfrac{\rho_0^g c_0^2}{k} \xi^2 f(\xi, n, c) \tfrac{\Delta_3}{\|a_{kl}\|} p_{r,n}^0,\\ M_{x,n}^0 = -\tfrac{ha}{12} \tfrac{\rho_0^g c_0^2}{k} \tfrac{i\xi\Delta_4 + n\nu\Delta_5}{\|a_{kl}\|_n} p_{r,n}^0,\\ Q_{x,n}^0 = -\tfrac{1-\nu}{2} \chi_0^2 a\, p_{r,n}^0 \tfrac{i\xi\chi\Delta_3\Delta_4}{\|a_{kl}\|}.\end{gathered}$$

Using (12), one can determine the transforms of the contact pressure, as well as the components of the stress-strain state of the core and the shell.

Let us write out the final formulas for a system of l concentrated, self-equilibrated forces uniformly distributed along the circumference:

$$p_r(\eta, \theta) = p_3 \delta(\eta) \sum\nolimits_{k=1}^{l} \delta\left(\theta - \theta_k\right). \tag{13}$$

If we assume that $p_3 = 2\pi p_0 / l$, where p_0 is the intensity of a uniformly distributed load along the circumference, then for the shell deflections and the contact pressure we can write

$$w^\star = \frac{2Gw}{p_0} = \frac{2(1-\nu)}{kl} \sum\nolimits_{n=0}^{\infty} \left[\int_0^\infty \frac{\cos(\xi\eta)\, d\xi}{F(\xi, n, c)}\right] a_n \cos(n\theta); \tag{14}$$

$$\sigma^\star = \frac{\sigma_{rr}|_{r=a}}{p_0} = -\frac{1-\nu}{kl\gamma} \sum\nolimits_{n=0}^{\infty} \left[\int_0^\infty \frac{f_1(\xi, n, c) \cos(\eta\xi)\, d\xi}{F(\xi, n, c)}\right] a_n \cos(n\theta); \tag{15}$$

$$F(\xi, n, c) = \frac{\nu\xi^2}{z_1} \left[(1+\nu) n z_4 - \nu\right] + 2n z_4 - z_3;$$

$$z_1 = d_{11}; \quad z_2 = d_{22}; z_3 = d_{33}; \quad z_4 = \frac{2z_1 n + \nu(1+\nu) n \xi^2}{4 z_1 z_2 + (1+\nu)^2 n^2 \xi^2}.$$

a_n are the Fourier coefficients of the function $\sum_{k=1}^{l} \delta\left(\theta - \theta_k\right)$.

In the calculations, the delta function was represented by a finite Fourier series with improved convergence [35]

$$\delta(\theta) = \frac{1}{\pi}\left[0.5 + \sum\nolimits_{n=1}^{N-1} \frac{N}{n\pi} \sin\left(\frac{n\pi}{N}\right) \cos(n\theta)\right]. \tag{16}$$

Taking (16) into account, the coefficients a_n in (14) and (15) take the form

$$a_n = \begin{cases} \frac{l}{2\pi},\ n = 0\ (l = 2, 4, \ldots\ldots), \\ \frac{lN}{n\pi^2} \sin\left(\frac{n\pi}{N}\right),\ n = lj, \\ 0,\ n \neq lj\ (j = 1, 2, \ldots) \end{cases}$$

3. Stationary response of the "cylindrical shell–viscoelastic core" system to the action of a moving load

In the problems considered above, the core or the medium surrounding the shell was assumed to be viscoelastic. At the same time, many cores encountered in practice are polymers with pronounced viscoelastic properties. Here, using the correspondence principle between the elastic and viscoelastic problems (the elastic-viscoelastic analogy) [34], a stationary solution is obtained for the problem of the action of moving loads on a cylindrical shell with a viscoelastic core. It is shown that this principle allows the previously considered problems of this class to be generalized to the case of viscoelastic media. Since the viscoelastic core has damping properties, the inversion integrals have no singularities on the real axis, and the elements of the determinants in the integrands become complex, since in this problem, in the transform space, the Lame coefficients are complex and depend on the load velocity and the parameter of the Fourier transform.

Let us write the equations of motion of the medium in a rectangular Cartesian coordinate system:

$$\sigma_{ij}(t) = \rho_c \frac{\partial^2 u_i}{\partial t^2}(i, j = x, y, z). \tag{17}$$

The relation between the components of the stress and strain tensors, in the case of differential operators, is taken in the form

$$\bar{\sigma}_{ij} = \widetilde{\lambda}\widetilde{\varepsilon}_{kk}\delta_{ij} + 2\widetilde{\mu}\widetilde{\varepsilon}_{ij}; \tag{18}$$

where

$$\lambda_0 f(t) = \frac{\nu_n \widetilde{E}_0 f(t)}{(1+\nu)(1-2\nu)}; \qquad \mu_0 f(t) = \frac{\nu \widetilde{E}_0 f(t)}{2(1+\nu)},$$

$\widetilde{E}_n$ is the operator modulus of elasticity has the form:

$$\widetilde{E}_n^0 f(t) = E_{0n}\left[f(t) - \int_0^t R_{E_n}(t-\tau) f(\tau)\, d\tau\right],$$

Here, δ_{ij} is the Kronecker delta, ρ_c is the density of the core, $f(t)$ is an arbitrary function of time, and *n* is Poisson's ratio.

The relations between the strains and the displacements have the form [5,35]

$$2 \ni_{ij} (t) = u_{ji}(t) + u_{ij}(t). \tag{19}$$

Let us write the boundary conditions for the viscoelastic body in the form

$$\begin{aligned} \sigma_{ij}(t) n_j = S_i J(t) \qquad &\text{on} \qquad \Gamma_\sigma; \\ u_i(t) = \Delta_i(t) \qquad &\text{on} \qquad \Gamma_u, \end{aligned} \tag{20}$$

where n_j are the components of the unit outward normal to the boundary of the body; Γ_σ is the part of the boundary on which the components of the stress tensor are given, and Γ_u is the part of the boundary on which the components of the displacement vector are given.

Let us pass from (16)–(18) to the moving coordinate system. Let the given loads, the sought displacements, and the stresses in the medium satisfy the conditions for the existence of the Fourier transform with respect to the variable η. Then, applying the Fourier transform to (16)–(18), in the transform space we obtain

$$\sigma_{ij,j}^{0} = -p_c \frac{c^2}{a^2} \xi^2 u_i^0; \tag{21}$$

$$\sigma_{ij}^{0} = \lambda(c,\xi)\delta_{ij} \ni^0 + 2\mu(c,\xi) \ni_{ij}^0 . \tag{22}$$

Here, $\lambda(c,\xi)$, $2\mu(c,\xi)$ are the complex Lame coefficients, depending on the velocity of motion and the parameter of the Fourier transform, determined by the formulas

$$\lambda(c,\xi) = \frac{Q_1^0(c,\xi)}{Q_0^0(c,\xi)}; \mu(c,\xi) = \frac{Q_2^0(c,\xi)}{2Q_0^0(c,\xi)}; \tag{23}$$

$$\begin{gathered} Q_0^0 = \textstyle\sum_{k=0}^{n_0} a_k \left(-\frac{c}{a}\right)^k (-i\xi)^k; \qquad Q_1^0 = \sum_{k=0}^{n_0} b_k \left(-\frac{c}{k}\right)^k (-i\xi)^k; \\ Q_2^0 = \textstyle\sum_{k=0}^{n_2} c_k \left(-\frac{c}{a}\right)^k (-i\xi)^k. \end{gathered} \tag{24}$$

Instead of (19) and (20), we have

$$2\epsilon_{ij}^0 = u_{i,j}^0 + u_{j,i}^0; \tag{25}$$

$$\sigma_{ij}^0 n_j = S_j^0 \text{ at } \Gamma_\sigma;\ u_j^0 = \Delta_i^0 \text{ at } \Gamma_u \tag{26}$$

Moreover, Γ_σ and Γ_u do not change, remaining unchanged together with the moving coordinate system.

The solution of the stationary problem of the action of a moving load on a viscoelastic medium can be obtained on the basis of the correspondence principle [36], according to which, in the transform space, in the formulas for the displacements and stresses of points of the elastic medium, the Lame coefficients must be replaced by complex coefficients, and then the final solution is obtained by the inverse Fourier transform. The main restriction in using this principle is the requirement that the surface parts Γ_σ and Γ_u do not change with time, which, in problems with moving loads, is postulated as the invariance of these regions in the moving coordinate system. In Safarov et al.'s research [36], when studying the action of a moving load on a multilayer viscoelastic foundation, the integral form of the relation between stresses and strains was used. It is shown that in this case, in the moving coordinate system, the displacements and stresses likewise do not depend on time, and the complex Lame coefficients can be obtained from the formulas

$$\begin{aligned} \lambda(c,\xi) &= \lambda_0 \left[1 - \textstyle\int_0^\infty f_1(t) e^{-ic\theta} dt\right]; \\ \mu(c,\xi) &= \mu_0 \left[1 - \textstyle\int_0^\infty f_2(t) e^{-ic\xi t} dt\right], \end{aligned} \tag{27}$$

where $f_1(t),\ f_2(t)$ are the kernels of the viscoelastic operators, which are functions of the bulk and shear relaxation rates.

Let us apply the method described above to solving the problem of the action of a moving load on an infinitely long cylindrical shell containing a viscoelastic core whose inner surface is free of stresses. Passing to the moving coordinate system and applying the Fourier transform with respect to η, in the transform space, we will seek the solution as Fourier series in the angular coordinate θ. Similarly, for determining $u_n^0, v_n^0, \omega_n^0, \psi_{x,n}^0, \psi_{y,n}^0$ a system of algebraic equations is obtained, which includes the Fourier coefficients of the transforms of the core reaction $q_{xc,n}^0, q_{\theta c,n}^0, q_{rc,n}^0$. In the modified (7), in this case

$$\begin{gathered} M_p(c,\xi) = c/c_p(c,\xi); M_s(c,\xi) = c/c_s(c,\xi); \\ c_p^2(c,\xi) = \frac{[\lambda(c,\xi)+2\mu(c,\xi)]}{p_c}; c_s^2(c,\xi) = \frac{\mu(c,\xi)}{p_c}. \end{gathered} \tag{28}$$

Here c_p, c_s are the propagation velocities of the tension-compression and shear waves in the core.

The further course of the solution is analogous to the case of an elastic core and can be carried out in two ways: 1) determine, from the boundary conditions, the relation between the core reactions and the transforms of the shell displacements, and obtain the final solution by resolving the above system of equations with respect to $u_n^0, \ldots, \psi_{y,n}$ (this approach is usually convenient for a solid core); 2) determine, from the system of algebraic equations, the loads transmitted to the core by the shell, expressing them in terms of the displacements, and rewrite the boundary conditions taking the formulas obtained into account. In this case, the final solution is obtained by satisfying the boundary conditions (this approach is used for shells with a hollow core and for three-layer shells).

As an example, numerical results are obtained for the problem of the motion of an axisymmetric normal load. Using the second approach to solving the problem and assuming that the contact between the shell and the core is sliding but the bond is bilateral, we determine the normal load transmitted to the core from the shell, with the addition of the transform of the given load. Writing the general solutions of (21) at $n = 0$ in the form (9) and then satisfying the boundary conditions, we arrive at a system of algebraic equations for determining the functions $A(\xi), \ldots, D(\xi)$, the solution of which is given by formulas of the form (12), taking into account that the elements of the determinant (13) include the complex Lame coefficients. If the core is solid, then the transforms of the displacements in the core are given by formulas of the form

$$u_r^0 = \frac{p_{r2}^0(\xi)a}{\mu(c,\xi)F_6(c,\xi)} \left[\left(M_s^2-2\right) J_1\left(\bar{m}_s\xi\right) J_1\left(\bar{m}_s\xi r_\star\right) + 2J_1\left(\bar{m}_s\xi\right) J_1\left(\bar{m}_s\xi r_\star\right)\right], \tag{29}$$

$$\begin{gathered} \sigma_{rr}^0 = \frac{p_{r2}^0(\xi)}{F_6(c,\xi)}\left\{\frac{M_s^2-2}{\bar{m}}\left[\left(\frac{\lambda(c,\xi)}{\mu(c,\xi)}M_p^2 + 2m^{-2}\right)\xi J_0\left(\bar{m}\xi r_\star\right) - \frac{2\bar{m}}{r_\star}J_1\left(\bar{m}\xi r_\star\right)\right]\right. \\ \left.\times J_1\left(\bar{m}_s\xi\right) + 4\left[\bar{m}_s\xi J_0\left(\bar{m}_s\xi r_\star\right) - \frac{1}{r_\star}J_1\left(\bar{m}_s\xi r_\star\right)\right] J_1\left(\bar{m}\xi\right)\right\}, \end{gathered} \tag{30}$$

$$F_6(c,\xi) = 2d_4 J_1\left(\bar{m}_s\xi\right) - \frac{\left(M_s^2-2\right) d_3 J_1\left(\bar{m}_s\xi\right)}{\bar{m}}; \tag{31}$$

$$\begin{gathered} d_3 = \left[\frac{\lambda(c,\xi)}{\mu(c,\xi)}M_p^2 + 2m^{-2}\right]\xi J_0\left(\bar{m}\xi\right) - \left(2-t_7\right)\bar{m}J_1\left(\bar{m}\xi\right); \\ d_4 = -2\bar{m}_s\xi J_0\left(\bar{m}_s\xi\right) + \left(2-t_7\right) J_1\left(\bar{m}_s\xi\right); \\ t_7 = \frac{2Gk\eta_4}{(1-\nu)\mu(c,\xi)}. \end{gathered} \tag{32}$$

The final solution is obtained by means of the inverse Fourier transform. Calculations were carried out for a ring concentrated load and a shell with a solid core for the following values of the dimensionless parameters:

$$k = 0,02; \qquad \nu = 0,3; \qquad \gamma = G/\mu_m^e = 125; \qquad p^\star = p/p_c = 12.5;$$
$$\lambda_m^\star = \lambda_m^e/\mu_m^e = 1.5; \qquad \tau_1^\star = \tau_1/\Omega = 0.25; \qquad \tau_2^\star = \tau_1/\tau_2 = 2.$$

The dimensionless velocity of load motion c_0 and the dimensionless characteristic of the uniaxial-strain recovery time $c_2^* = c_{se}/ar \left(c_{se} = (\mu_m^e/p_c)^{1/2}\right)$ were varied.

4. Results and discussion

To account for the viscoelastic properties of the material, the Rzhanitsyn–Koltunov kernel was adopted: $R_{En}(t) = \frac{A_n e^{-b_n t}}{t^{1-a_n}}$, with parameter values $A_1 = 0.048$; $b_1 = 0.05$; $a_1 = 0.10$; $A_2 = 0.078$; $a_1 = 0.15$. In the calculations, the following values of the dimensionless parameters were adopted: $k = 0.02; v = v_c = 0.025; p^* = 12.5$.

Analysis of the dispersion curves (see **Figure 1**) shows that the difference between the velocities of the axisymmetric and non-axisymmetric waves of the first mode is small for all values of the wave number, except those close to zero (the region of very long waves), and the minima of the first-mode curves for all values of *n* coincide, so that in this case too the first resonance velocity can be determined from the solution of the corresponding axisymmetric problem. Thus, for $\gamma = 250$ the value obtained is $c_* = 0.31 \left(3\rho/\bar{G}\right)^{1/2}$. Further analysis is restricted to pre-resonance velocities of motion ($c < c_\phi$). In this case, the improper integrals in (12) and (13) are not singular, and the numerical results are obtained using the MATLAB software package.

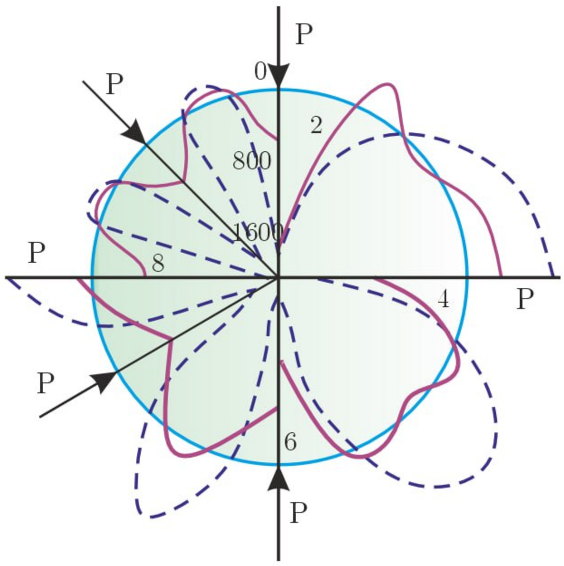

Figure 1. Variation of the shell deflections around the circumference.
Note: Dashed lines indicate the unfilled shell; solid lines indicate the filled shell.

Figure 1 shows the distribution of the dimensionless shell deflections w^* around the circumference, in the cross-section $\eta = 0$, for two, four, six, and eight concentrated forces (11) at $\gamma = 250, c_0 = 0.1$. The dashed lines relate to the shell without a core, and for clarity, a separate scale, different from that used for the shell with the core, is chosen for each such curve. As shown in **Figure 1**, the presence of the core significantly influences the pattern of the deflection distribution, especially for two and four forces. As the number of forces increases, the influence of the core on the qualitative pattern of the deflection variation around the circumference decreases.

Figure 2 illustrates the variation of the contact stresses σ^* in the same cross-section and for the same parameter values. As can be seen from **Figure 2**, compressive contact stresses occur only in a certain neighborhood of the point of application of each force. As one moves away from the point of application of the force around the circumference, the stresses change sign in all the cases considered. This is a consequence of the assumption of a bilateral bond between the shell and the core. If the bond is assumed to be unilateral, it becomes possible for the bond to be released in those regions where tensile stresses arise, resulting in separation of the shell from the core.

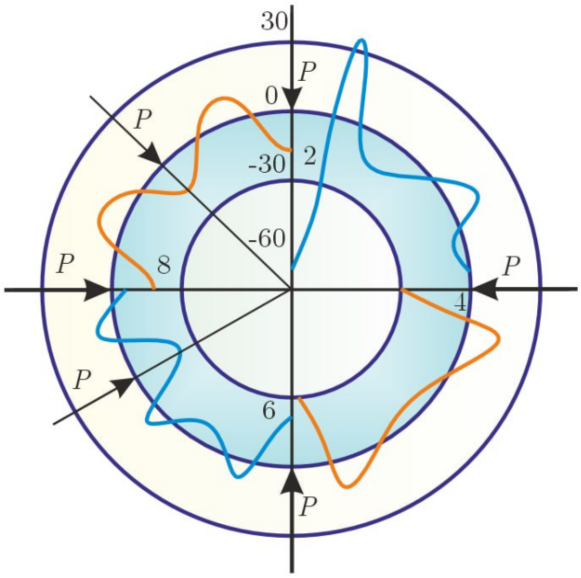

Figure 2. Contact stresses at the boundary between the shell and the core for different numbers of concentrated forces.

Note: Solid lines denote the filled shell (orange line—contact stresses for two applied forces, blue line—contact stresses for four applied forces).

Figure 3 shows the distribution of the radial displacements, and **Figure 4** the radial stresses σ^* across the thickness of the core for various cross-sections η = const in the axisymmetric case (n = 0) for various values of the relative stiffness (1—$\gamma = 250$; 2—$\gamma = 120$; 3—$\gamma = 60$).

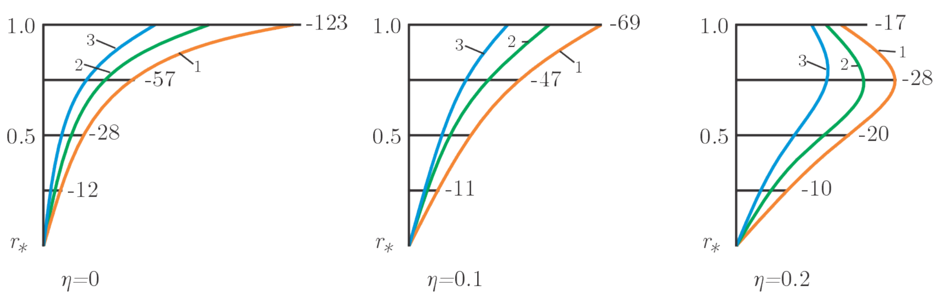

Figure 3. Distribution of the radial displacements across the thickness of the core.

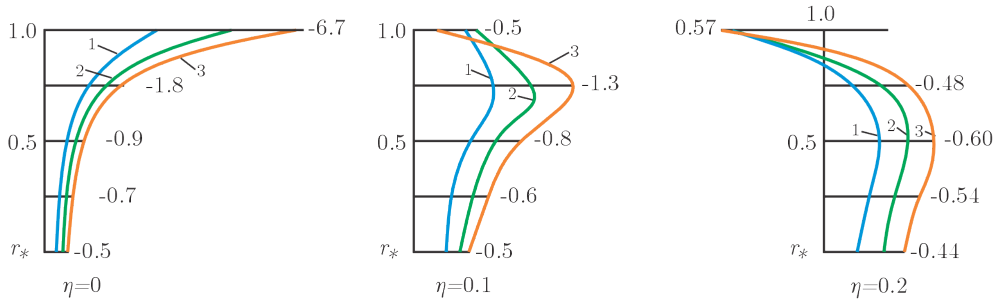

Figure 4. Radial stresses at points of the core for various distances from the point of loading.

For clarity, a separate scale is chosen for each cross-section.

As can be seen from the figures, moving away from the point of load application along the length of the shell, the character of the distribution changes substantially, especially for the stresses. Moreover, whereas for cross-sections $\eta = 0$ and $\eta = 0.1$, all the stresses are compressive, already for cross-section $\eta = 0.2$ in the part of the core adjoining the shell, tensile stresses appear. Thus, separation of the shell from the core can occur not only around the circumference but also along the length, and the variation of the core stiffness within the range considered here has little effect on the length of the contact zone. Taking the viscosity of the materials into account slightly reduces the stresses and displacements of the core and the shell.

Owing to the damping properties of the viscoelastic core, the stationary solution obtained is unique for any velocity of load motion. The inversion integrals are not singular, and their values are found by Filon's method.

Figure 5 shows the distribution of the dimensionless deflections.

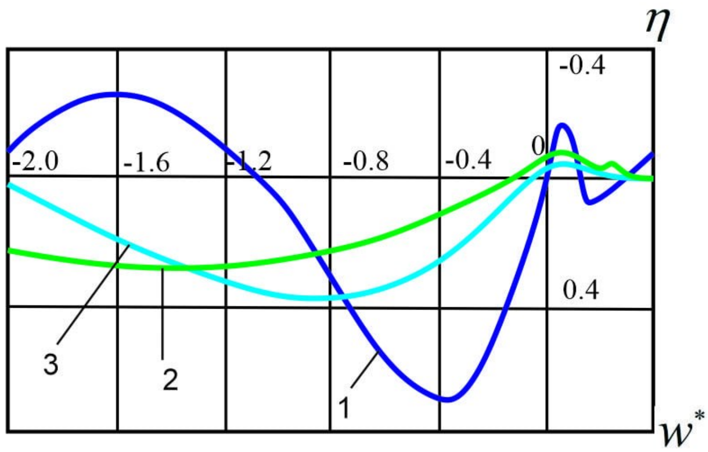

Figure 5. Deflections of the shell with a viscoelastic core for various regimes of motion of the ring load.

Note: For the given curve 1—$c_0 = 0.6$; for the given curve 2—$c_0 = 1.2$; for the given curve 3—$c_0 = 1.8$. $\omega^* = -2G\omega/p_0$ along the length of the shell for various velocities of motion of the ring load, with the solid lines relating to the shell.

As can be seen from **Figure 5**, as the load velocity increases, the maxima of the deflections decrease and their lag behind the load front increases. Within the range of velocities considered, on the trailing wave, the results of both shell theories coincide, and a difference in the deflections is observed only at $c_0 = 0.6$ the leading wave.

Figure 6 illustrates the variation of the contact pressure $\sigma^* = \sigma_{\gamma\gamma}|_{\gamma=a}a/p_0$ at the boundary of the "shell–viscoelastic core" system. The calculations show that, for

$c_0 = 0.6$, taking transverse shear and rotary inertia into account has a substantial effect on the results. Unlike the deflections, the maxima of the contact stresses lag less behind the load front.

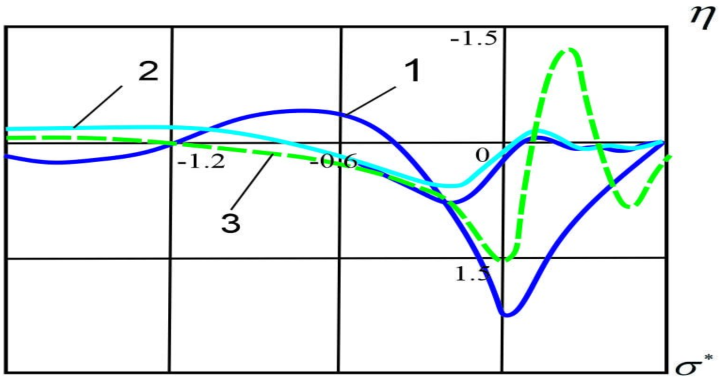

Figure 6. Contact stresses at the boundary of the "shell–viscoelastic core" system according to Timoshenko theory, with the dashed lines relating to the Kirchhoff–Love shell.

Note: For the given curve 1—$c_0 = 0.6$; for the given curve 2—$c_0 = 1.2$; for the given curve 3—$c_0 = 1.8$.

The variation of the contact stress ($\sigma^* = \sigma_{\gamma\gamma}|_{\gamma=R_1}/\sigma_0$), which arises in the core, is shown in **Figures 7** and **8**. **Figure 7** shows that as the load velocity increases, the contact pressure decreases moderately. The graphs show that as the viscosity amplitude increases, the contact stresses decrease.

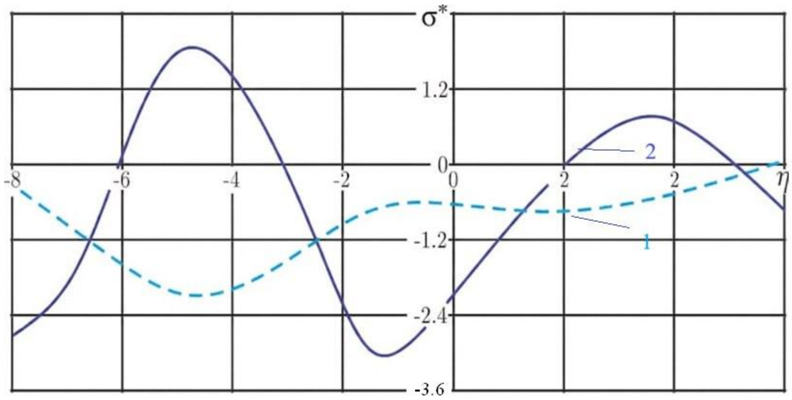

Figure 7. Contact stresses at the boundary of the "shell–viscoelastic core" system.

Note: The dashed line corresponds to the shell of Kirchhoff–Love, the solid line to the three-dimensional theory of viscoelasticity. 1—$c_0 = 1.2$; 2—$c_0 = 0.5$.

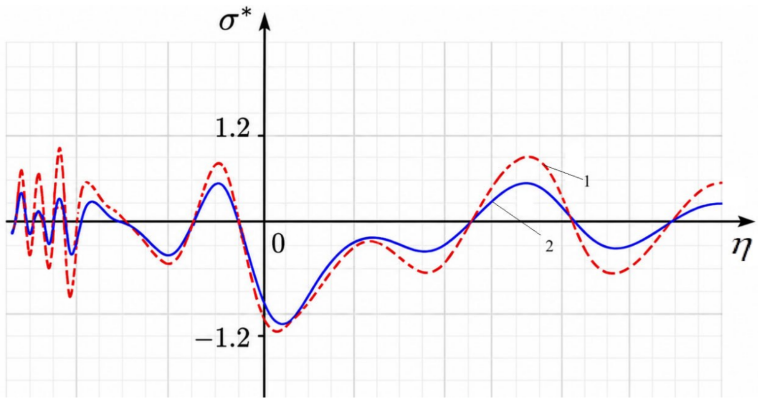

Figure 8. Contact stresses at the boundary of the "shell–viscoelastic core" system.

Note: The dashed line corresponding to the three-dimensional theory of viscoelasticity. 1—$A = 0.001$, $c_0 = 0.45$; 2—$c_0 = 0.04$.

In conclusion, we note that taking the viscoelastic properties of the core into account makes it possible to treat all regimes of load motion uniformly from the point of view of computing the inversion integrals.

5. Conclusion

The paper presents the problem statement, the calculation methods, and numerical results for the response of a cylindrical shell with a solid viscoelastic core to a non-axisymmetric moving load. Numerical results have been obtained, on the basis of which it is established that:

- Moving away from the point of load application along the length of the shell, the distribution pattern changes substantially, especially for the stresses;
- Separation of the shell from the core can occur not only around the circumference but also along the length, and the variation of the core stiffness within the range considered here has little effect on the length of the contact zone.

Author contributions: Conceptualization, ZB and NE (Nuriddin Esanov); methodology, ZB, NE (Nuriddin Esanov) and SJ; software, RS, GM and US; validation, SK, A.J. and S.O.; formal analysis, ZB, SJ and KK; investigation, RS, GM, US and NE (Nazokat Ergasheva); resources, SK, A.J., S.O., K.K. and NE (Nazokat Ergasheva); data curation, US, Sk and AJ; writing—original draft preparation, ZB, NE (Nazokat Ergasheva) and SJ; writing-review and editing, ZB, SJ and RS; visualization, GM, SO and KK; supervision, ZB and SJ; project administration, ZB; funding acquisition, ZB. All authors have read and agreed to the published version of the manuscript.

Funding: This work received no external funding

Institutional review board statement: Not applicable. This study did not involve human participants or animals.

Informed consent statement: Not applicable.

Data availability statement: The data used in this study are available from the corresponding author upon reasonable request.

Conflict of interest: The authors declare that they have no competing interests.

AI use statement: The authors declare that no artificial intelligence (AI) tools were used in the preparation of this manuscript.

References

1. Akhenbach D. Moving load applied to a plate on an elastic half-space. Prikladnaya Mekhanika. 1967; (4): 83–88. (in Russian)
2. Mindlin RD. Influence of rotatory inertia and shear on flexural motions of isotropic elastic plates. Journal of Applied Mechanics. 1951; 18: 31–38.
3. Novatskiy V. Theory of Elasticity. Mir Publishers; 1975.

4. Gao G, Sun N, Shao D, et al. Forced and post-forced responses of multi-stepped composite cylindrical shell under general moving excitations. Thin-Walled Structures. 2024; 198: 111734. doi: 10.1016/j.tws.2024.111734
5. Li YP, She GL. Nonlinear dynamic response of graphene platelets reinforced cylindrical shells under moving loads considering initial geometric imperfection. Engineering Structures. 2025; 323: 119241. doi: 10.1016/j.engstruct.2024.119241
6. Ghugal YM, Shimpi RP. A review of refined shear deformation theories of isotropic and anisotropic laminated plates. Journal of Reinforced Plastics and Composites. 2002; 21(9): 775–813. doi: 10.1177/073168402128988481
7. Nasrekani FM. A closed-form solution for dynamic analysis of auxetic sandwich cylindrical structures with FG face sheets under moving pressure. Mechanics Based Design of Structures and Machines. 2025; 53(10): 6789–6807. doi: 10.1080/15397734.2025.2490808
8. Konoplev YG, Yakushev RS. Lectures on the Dynamics of Structures under Moving Loads. Otechestvo, Kazan; 2003. (in Russian)
9. Cai Y, She GL. Nonlinear dynamic response of magneto-electro-elastic cylindrical shells subjected to moving load. Mechanics of Advanced Materials and Structures. 2026; 33(1). doi: 10.1080/15376494.2025.2463090
10. Zhao X, Sun S, Chu S, et al. Multi-mode vibration control and optimization of smart rotating cylindrical shells subjected to circumferential moving loads. Thin-Walled Structures. 2025; 211: 113094. doi: 10.1016/j.tws.2025.113094
11. Firsanov VV. The stressed state of "boundary layer" type cylindrical shells investigated according to a nonclassical theory. Journal of Machinery Manufacture and Reliability. 2018; 47: 241–248. doi: 10.3103/S1052618818030068
12. Firsanov VV, Vo AK. The study of the longitudinally stiffened cylindrical shells under action of local load by the refined theory. Proceedings of Moscow Aviation Institute. 2018; (102). (in Russian)
13. Firsanov VV, Vo AK, Chan ND. Studying stiffened shells stress state by the refined theory with account for ribs elasticity and clamped edge. Proceedings of Moscow Aviation Institute. 2019; (104). (in Russian)
14. Zhou F, Chen Z, Fan H, et al. Analytical study on the buckling of cylindrical shells with stepwise variable thickness subjected to uniform external pressure. Mechanics of Advanced Materials and Structures. 2016; 23(10): 1207–1215. doi: 10.1080/15376494.2015.1068401
15. Auersch L. The effect of the critically moving loads on the vibrations of soft soils and isolated railway tracks. Journal of Sound and Vibration. 2008; 310(3): 587–607.
16. Karpov VV, Ignatiev OV, Semenov AA. Stress-strain state of ribbed shell structures. Magazine of Civil Engineering. 2017; 6(74): 147–160. doi: 10.18720/MCE.74.12
17. Wang H, Chen Y, Xi Z, et al. Forced vibration of sandwich pipes with zero Poisson's ratio honeycomb core under moving pressure. International Journal of Pressure Vessels and Piping. 2023; 202: 104876. doi: 10.1016/j.ijpvp.2022.104876
18. Hussein MFM, Hunt HEM. Modeling of floating-slab tracks with continuous slabs under oscillating moving loads. Journal of Sound and Vibration. 2006; 297(1–2): 37–54.
19. Bahranifard F, Malekzadeh P, Golbahar Haghighi MR. Moving load response of ring-stiffened sandwich truncated conical shells with GPLRC face sheets and porous core. Thin-Walled Structures. 2022; 180: 109984. doi: 10.1016/j.tws.2022.109984
20. Safarov I, Nuriddinov B, Nuriddinov Z. Propagation of own waves in a viscoelastic cylindrical panel of variable thickness. Lobachevskii Journal of Mathematics. 2024; 45: 1246–1253. doi: 10.1134/S1995080224600663
21. Safarov I, Teshaev M. Control of resonant oscillations of viscoelastic systems. Theoretical and Applied Mechanics. 2024; 51(1): 1–12.
22. Akbarov D, Mehdiyev MA. Forced vibration of the elastic system consisting of the hollow cylinder and surrounding elastic medium under perfect and imperfect contact. Structural Engineering and Mechanics. 2017; 62(1): 113–123.
23. Teshaev MK, Safarov II, Kuldashov NU, et al. On the distribution of free waves on the surface of a viscoelastic cylindrical cavity. Journal of Vibration Engineering & Technologies. 2020; 8: 579–585.
24. Pan H, Hu Y, Liu S. Sandwich cylindrical shells with a porous E-FGM core and FG-CNTRC face sheets undergoing harmonic base-acceleration load. Mechanics Based Design of Structures and Machines. 2026; 54(1). doi: 10.1080/15397734.2026.2617882
25. Hasheminejad M, Komeili M. Effect of imperfect bonding on axisymmetric elastodynamic response of a lined circular tunnel in poroelastic soil due to a moving ring load. International Journal of Solids and Structures. 2009; 46(2): 398–411.
26. Girnis SR. Action of a moving load on a two-layer shell in an elastic medium. In: Beskopylny A, Shamtsyan M,

Artiukh V (editors). Proceedings of XV International Scientific Conference INTERAGROMASH 2022. Lecture Notes in Networks and Systems. Springer; 2023. 574, pp. 2301–2311.
27. Zhou YB, Li XF. Fracture analysis of an infinite 1D hexagonal piezoelectric quasicrystal plate with a penny-shaped dielectric crack. European Journal of Mechanics—A/Solids. 2019; 76: 224–234.
28. Rao KRM, Rao PH, Chaitanya BSK. Piezoelectricity in quasicrystals: A group-theoretical study. Pramana Journal of Physics. 2007; 68(3): 481–487.
29. Yang LZ, Gao Y, Pan E, et al. Electric-elastic field induced by a straight dislocation in one-dimensional quasicrystals. Civil Engineering Faculty Research. 2014; 126(2): 467–470.
30. Li XY, Li PD, Wu TH, et al. Three-dimensional fundamental solutions for one-dimensional hexagonal quasicrystal with piezoelectric effect. Physics Letters A. 2014; 378(10): 826–834.
31. Guo JH, Pan E. Three-phase cylinder model of one-dimensional hexagonal piezoelectric quasicrystal composites. Journal of Applied Mechanics. 2016; 83(8): 081007.
32. Safarov II, Akhmedov MS, Boltaev ZI. Setting the linear oscillations of structural heterogeneity viscoelastic lamellar systems with point relations. Applied Mathematics. 2015; 6(2): 228–234.
33. Gorshkov AG, Starovoitov EI, Yarovaya AV. Mechanics of Layered Viscoelastic-Plastic Structural Elements. FIZMATLIT; 2005.
34. Shi L, Selvadurai APS. Dynamic response of an infinite beam supported by a saturated poroelastic half-space and subjected to a concentrated load moving at a constant velocity. International Journal of Solids and Structures. 2016; 88–89: 35–55.
35. Safarov I, Teshaev M, Boltayev Z, et al. Propagation of unsteady waves in a layered cylinder. Archive of Applied Mechanics. 2025; 95(10): 239. doi: 10.1007/s00419-025-02943-z
36. Safarov II, Teshaev MK, Negmatillaev B, et al. Oscillations of a rigid strip on a viscoelastic half-plane under the vertical load. Tomsk State University Journal of Mathematics and Mechanics. 2025; (95). doi: 10.17223/19988621/95/13 (in Russian)